Designing Ephemeris Capture Trajectories at Europa Using Unstable Periodic Orbits

Ryan P. Russell[*] and Try Lam[†]

Jet Propulsion Laboratory, California Institute of Technology, Pasadena, California 91109

Europa's proximity to Jupiter creates a hostile dynamic environment for a spacecraft with limited control authority as is typical with low-thrust missions. The unstable third-body effects are magnified near the polar inclinations where science orbits reside, and plane changes deep within Europa's gravity well are fuel and time expensive. Therefore, designing capture trajectories directly to highly inclined states is desirable but challenging because of the pronounced instability and lack of thrust authority. The approach outlined here confronts this problem by using dynamical systems theory and an extensive preexisting database of restricted three-body problem periodic orbits. The stable manifolds of unstable periodic orbits are used to attract a spacecraft towards Europa. By selecting an appropriate periodic orbit, a mission designer can control important characteristics of the captured state including stability, minimum altitudes, characteristic inclinations, and characteristic radii, among others. Several free parameters are adjusted in the nontrivial mapping from the simplified to a more realistic model until a satisfactory ephemeris capture is found. Although the final capture trajectory is ballistic by design, low thrust is used to target the state that leads to the capture orbit, control the spacecraft after arriving on the unstable quasi-periodic orbit, and begin the spiral down towards the science orbit. Despite the limited control authority and the highly unstable dynamical environment, the method provides structure to the design process and enables the systematic targeting of ephemeris model capture state characteristics.

I. Introduction

TYPICAL science orbits at Europa require close proximity to the surface and high inclinations to provide global coverage for mapping purposes. Capturing directly to these orbits using low thrust is impossible because of the forbidden regions associated with the dynamics of the restricted three-body problem (RTBP). A capture trajectory with limited control authority is thus restricted to higher altitude orbit insertions. Furthermore, a host of recent studies has reemphasized that the high-inclination mapping orbits are unstable [1–5] and increasingly so at the higher altitudes where low-thrust captures are feasible.

Distant retrograde orbits (DROs) exist in the ephemeris model at Europa well beyond 50,000 km and are extremely stable when the out-of-plane motion is small [4]. As a result, a typical and rather straightforward approach for designing a capture orbit at Europa follows the path of inserting into a near-planar DRO and then systematically changing the characteristic radius and inclination until a science orbit is achieved [6–8]. Although this approach is inherently less risky, it can be costly both in time and fuel [8]. Thus, we proceed by outlining a capture technique that provides mission designers the improved ability to target a variety of close, highly inclined capture orbits with little thrusting capabilities even in the highly unstable regions of the design space.

Recent applications of dynamical systems theory to the multibody astrodynamics problem have led to a new paradigm of trajectory design [9–21]. From this perspective, trajectories exploit natural unstable dynamics to efficiently navigate through chaotic regions in phase space [20,22]. The perturbing effects of a secondary gravitating body in the vicinity of a primary body and a spacecraft can be used to capture or escape the primary using little or no fuel. The capture or escape trajectories follow stable or unstable manifolds of unstable periodic orbits. The set of these manifolds emanating from the Lagrange points mapped for the many attracting bodies in the solar system comprise what some researchers refer to as the *interplanetary superhighway* [23]. The paths of these manifolds meander through the solar system, and intersections of two manifolds provide mechanisms to ballistically connect two seemingly isolated regions [24]. Koon et al. [9] call the set of these low-energy passageways the "interplanetary network of dynamical channels." These efficient trajectory design concepts have been successfully demonstrated in flight missions such as International Sun-Earth Explorer-3 (ISEE-3), Advanced Composition Explorer (ACE), Solar and Heliospheric Observatory (SOHO), and Genesis, among others [25–29]. Notably, low-energy passageways in the Earth–moon system enabled the rescue of Japan's Hiten spacecraft when its nominal lunar mission failed [22].

Although the manifolds associated with the Lagrange point orbits have been the focus of most applications in this area, there are scores of other families of periodic orbits and associated invariant manifolds that have received much less attention. In this paper, we tap into this potential by using an extensive database of previously computed periodic orbits as attracting mechanisms for Europa capture [30]. Whereas Lo and Parker [14] investigate the manifolds and heteroclinic transfers therein of the simple planar RTBP periodic orbits (not limited to Lagrange point orbits), we extend the application here to consider nonsimple three-dimensional periodic orbits. Specifically, we employ a class of unstable highly perturbed two-body orbits that are periodic in the rotating frame after making several Europa revolutions. Because of the long periods and multiple revolutions, the structure of the manifolds of these more complicated periodic orbits is much more erratic in general than the manifolds that emanate from the simple Halo orbits [14,31]. Perhaps the individual trajectories that make up the complicated manifolds are more akin to one-lane county roads than a superhighway; nonetheless, they are capable of providing efficient ballistic captures to orbits with specific, selected characteristics.

Whereas the Halo orbit manifolds can certainly be used to initiate capture at Europa [8,11–13], powered maneuvers (albeit small) are

*Engineer, Guidance Control and Navigation, 4800 Oak Grove Drive, M/S 301-140L; Ryan.Russell@jpl.nasa.gov. Member AIAA.

†Engineer, Guidance Control and Navigation, 4800 Oak Grove Drive, M/S 301-125L; Try.Lam@jpl.nasa.gov. Member AIAA.
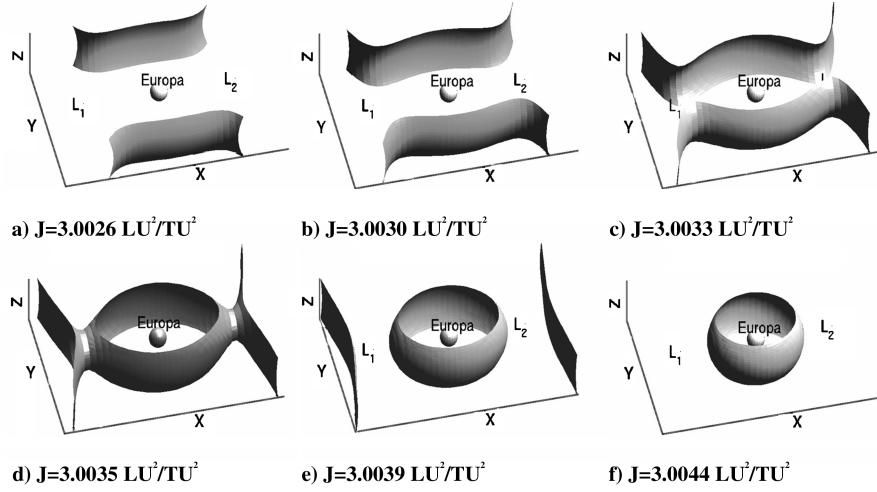
Fig. 1   Zero-velocity surfaces for Europa. The surfaces are sliced in order for Europa to be visible. The region of valid motion in a)–d) includes Europa and its Lagrange points, L1 and L2. After the neck closes from d) to e), the valid region near Europa is enclosed and thus isolated from the valid regions beyond the Lagrange points.

necessary to transfer the final capture state to one orbiting Europa rather than a Lagrange point. Furthermore, the unstable nature of the Lagrange points makes it difficult for a mission designer to control the final characteristics of the capture state. By using the manifolds of a Europa-centered periodic orbit directly, the dynamics are exploited to allow the spacecraft to naturally coast to its desired capture state. Using this approach, the important targeting maneuver is shifted from the chaotic regions near Europa to a safe distance well beyond its formal sphere of influence. Once captured, thrusting is reserved for controlling the spacecraft on the quasi-periodic ephemeris orbit, and finally for spiraling down to its final low-altitude science orbit.

The technique described in this paper is efficient in terms of spacecraft fuel because it allows for the design of close, highly inclined captures, thus reducing the need for expensive plane changes to achieve near-polar science orbits. Furthermore, the technique reduces design time because it is systematic and provides the trajectory designer control over the qualities of the capture state despite the generally chaotic dynamic environment.

We note that the ballistic capture trajectories sought currently are subsets of the broader classes of captures documented in [32] where Poincaré maps (instead of periodic orbits) are employed to find initial conditions that lead to safe captures. Whereas the current approach gives the designer more control over the specific characteristics of the resulting capture orbit, the use of the Poincaré maps provides a more global view of capture initial conditions.

The first section gives an overview of the relevant dynamics and models. The next section outlines the algorithm to systematically design a capture orbit at Europa using limited control authority. The initial conditions of several promising target periodic orbits are presented along with characteristics of the associated attracting trajectories.[‡] Although all of the target periodic orbits are unstable by design, some of the examples are selected because of their proximity to a recently observed class of direct, near-circular periodic orbits that are stable at surprisingly high inclinations [30,33]. The subtleties associated with mapping the simple model trajectories into a realistic model are explored, and a variety of parameters are introduced and optimized to ensure continuous ballistic captures in the full ephemeris model. Finally, we walk through an example application of a low-thrust transfer from Ganymede to a captured state at Europa.

II.   Background

The equations of motion for a nonthrusting spacecraft in the RTBP are presented in Eq. (1) in the standard rotating frame that assumes Europa and Jupiter orbit their common center of mass with a constant separation of 1 length unit (LU) and an orbital rate of 1 rad per time unit (TU). The coordinate frame is centered at Europa, the x-axis points along the Jupiter to Europa line, and the z-axis points toward the system angular momentum vector. The spacecraft distances to Europa and Jupiter are denoted as r_E and r_J, respectively. The gravitational parameters for Europa and Jupiter are Gm_E and Gm_J, respectively.

$$\mathrm{d}X/\mathrm{d}t = f(X) \qquad (1)$$

where

$$f = \begin{bmatrix} u \\ v \\ w \\ 2v + \partial\Omega/\partial x \\ -2u + \partial\Omega/\partial y \\ \partial\Omega/\partial z \end{bmatrix} \qquad X = \begin{bmatrix} x & y & z & u & v & w \end{bmatrix}^T$$

$$\Omega = (-x - 1 + \mu)^2/2 + y^2/2 + (1 - \mu)/r_J + \mu/r_E$$

$$\mu = Gm_E/(Gm_J + Gm_J) \qquad r_J = \sqrt{(x+1)^2 + y^2 + z^2}$$

$$r_E = \sqrt{x^2 + y^2 + z^2}$$

The Jacobi constant is an integral of motion for the RTBP and exists in the form given in Eq. (2). Therefore, the Jacobi constant (or energy) of a spacecraft can only be changed via thrusting.

$$J = 2\Omega - u^2 - v^2 - w^2 \qquad (2)$$

For the unthrusted case at a fixed value of J and velocity of zero, Eq. (2) can be solved for a surface in position space that represents the boundary between valid and forbidden regions for the spacecraft. This is known as the zero-velocity surface and is illustrated in Fig. 1. The neck seen in 1d is known as Hill's neck. When its radius shrinks to zero, ballistic transfers to and from the vicinity of Europa are no longer possible. Thus, for potential transfer orbits an upper bound is established for the Jacobi energy ($\sim$3.0036 LU^2/TU^2). This is equivalent to a lower bound on feasible ballistic capture orbit altitudes. At Europa, Hill's neck closes for inclined near-circular orbits when the radius is on the order of 5000 km [30]. Therefore, ballistic captures to near-circular orbits smaller than this threshold (i. e., after Hill's neck closes) are dynamically impossible.

[‡]The term "attracting trajectories" is used throughout and is indicative of a trajectory that is attracted to the target periodic orbit via the stable manifold. Because the attracting trajectories may not fall exactly on the invariant manifold, we often speak of the single trajectories to emphasize this difference.

Table 1   Jupiter–Europa RTBP parameters

Parameter	Symbol	Value	Comment
Europa gravitational parameter	Gm_E	$3,202.72 \text{ km}^3/\text{s}^2$	[34]
Jupiter gravitational parameter	Gm_J	$1.2668654 \times 10^8 \text{ km}^3/\text{s}^2$	[34]
Jupiter–Europa distance, length unit	LU	670,900 km	[34]
Europa mean radius	——	1,560.7 km	[34]
Mass ratio	μ	$2.52800260797625 \times 10^{-5}$	Calculated from Eq. (1)
Time unit	TU	48,822.0443306681 s	Calculated time for Europa to traverse 1 rad
Velocity unit	VU	13.7417432882581 km/s	Length unit divided by time unit

For the thrusting case, the spacecraft mass becomes a state variable and is governed by Eq. (3). The thrust acceleration term in Eq. (4) must be included in the velocity derivative terms given in the last three entries of f in Eq. (1). Note that Γ is the rocket thrust magnitude and the product $g_0 I_{sp}$ is the rocket exhaust velocity where I_{sp} is given in units of time and g_0 is the acceleration of gravity at the surface of Earth. Table 1 gives specific values for the RTBP parameters used in this paper for the Jupiter–Europa system. For details on the RTBP see, for example, [21,35].

$$\mathrm{d}\, m/\mathrm{d}t = -\Gamma/(g_0 I_{sp}) \tag{3}$$

$$\Gamma = \begin{bmatrix} \Gamma_x & \Gamma_y & \Gamma_z \end{bmatrix}^T / m \tag{4}$$

We proceed with a brief discussion on the stability of periodic orbits and an explanation why unstable periodic orbits share attracting and repelling qualities. A small perturbation, $\delta X(t_0)$, to the initial conditions of a ballistic reference trajectory, X^*, is linearly mapped forward to a perturbation at a later time with the well-known state transition matrix, Φ.

$$\delta X(t) = \Phi(t, t_0)\delta X(t_0) \tag{5}$$

The state transition matrix is obtained by integrating the variational equations given in Eq. (6). For a detailed derivation, see, for example, [36].

$$\dot{\Phi}(t, t_0) = (\partial f/\partial X)|_* \Phi(t, t_0) \qquad \Phi(t, t_0) = I \tag{6}$$

The Monodromy matrix, $\Phi(T, t_0)$, maps an initial state perturbation vector across one full period, T [37]. An eigenvalue, λ (real or complex), of the Monodromy matrix is a scalar proportionality factor that satisfies the relation

$$\Phi(T, t_0)\xi = \lambda \xi \tag{7}$$

For an eigenvalue with a magnitude greater than unity, perturbations in the eigendirection, ξ, will grow after one period, and the orbit is unstable in this direction. It is well known that the eigenvalues of the Monodromy matrix of a Hamiltonian system occur in reciprocal pairs [38]. Additionally, one of the eigenvalues will be unity for the autonomous system due to the preservation of the orbit in the tangent direction [21,37,38]. The eigenvalues of the Monodromy matrix for the three-dimensional RTBP will therefore have the form $\{\lambda_1, 1/\lambda_1, \lambda_2, 1/\lambda_2, 1, 1\}$. Thus, if a periodic orbit has an eigendirection that leads to an expansion, then there is also an accompanying eigendirection that leads to a contraction. Therefore, all eigenvalues must have a magnitude of 1 for stability in all six directions, and lastly, all unstable periodic orbits have directions that lead to both attracting and repelling trajectories.

A stable or unstable manifold is composed of trajectories that approach or leave in forward time a periodic orbit in the direction of a stable or unstable eigendirection, respectively. From Eq. (7), it is clear that the degree of stability or instability is reflected in the magnitude of the associated eigenvalue, where values less or greater than unity are increasingly stable or unstable, respectively. Although

the unstable manifolds are equally useful for general mission design, the remainder of this study focuses on the stable manifolds and their application to capture orbits.

III.   Ephemeris Model Considerations

The RTBP model is convenient because it enables fast numerical analysis and accurately represents to first order the motion of many real three-body systems. In addition, its autonomous Hamiltonian nature leads to many niceties including the abundant existence of periodic orbits, the availability of an integral of motion, and a simplified Monodromy matrix. However, in general, the difference between the RTBP and a more realistic model is not trivial. Surprisingly, much of the astrodynamic research applied to dynamical systems theory fails to include this final step of finding the trajectories in a full ephemeris model. In this paper, careful attention is paid to the ephemeris model by optimizing over several mapping parameters such that the final capture orbits are ballistic in the more realistic model.

The typical approach for continuing a RTBP solution to the ephemeris model involves breaking the trajectory into several legs and mapping the initial conditions for each leg to the ephemeris model. Next, a multiple shooting method is implemented using a differential corrector and/or optimizer to drive the ephemeris model legs towards continuity [19,21]. Some researchers have implemented least-squares techniques to aid in this transformation [21]. Of course, the techniques are equally useful for the inverse problem of obtaining a simplified trajectory starting from one in a full ephemeris [11,12]. In some cases, it may be necessary to parametrically solve several subproblems of increasing or decreasing complexity until a solution is found in the desired model [11,12]. The multiple shooting and homotopy techniques are increasingly difficult for long and complicated trajectories, and there is no guarantee that a completely ballistic ephemeris trajectory exists, especially in cases where the physical models are not as well represented by the assumptions of the RTBP. These common approaches preserve the trajectory shape even for highly unstable orbits.

Here, an alternative approach is taken that does not necessarily preserve the trajectory shape, but removes the necessity for multiple legs and ensures continuity, i.e., a ballistic capture. Note that a captured state in this context is a loosely defined term meaning that the spacecraft is on an ephemeris version of a ballistic trajectory associated with the stable manifold of the RTBP periodic orbit. Depending on the stability characteristics of the target periodic orbit, a spacecraft on the orbit, if left uncontrolled, will typically complete on the order of a few revolutions around Europa before falling off onto one of its unstable manifolds. For the present application, the target periodic orbit is employed only as a mechanism to achieve some intermediate captured state near Europa with important but loosely defined qualities, such as characteristic radii, inclination, and minimum and maximum altitudes. It is not critical that the final ephemeris capture trajectory be exactly analogous to its cousin orbit in the RTBP. Rather, it is only important that the qualities are similar and that the ephemeris trajectory does indeed ballistically follow a stable manifold towards a captured (albeit unstable) state at Europa.

The proposed mapping from a normalized RTBP state to a dimensioned state in the true ephemeris consists of two steps: first, unnormalizing the state in the RTBP, and second, doing the appropriate rotations to a nonrotating state. Typically, the normalized RTBP position and velocity vectors are dimensioned using the length unit and velocity unit (VU) given in Table 1. We propose a slight variation that provides a degree of freedom in the mapping. The distance from Jupiter to Europa in reality varies on the order of a few percent of its nominal value. Among many of the nonautonomous forcing functions that drive a real ephemeris, this pulsating feature of the radius introduced by a noncircular orbit is the largest perturbation to the assumptions of the RTBP. The length unit from Table 1 represents the average value of this pulsating radius. To account for the few percent in variation, we introduce a k scaling factor in Eq. (8) that provides new length units, time units, and velocity units for a RTBP system with a slightly modified characteristic length. The time and velocity units do not scale linearly because they are derived from the length unit. By varying k from 0.97 to 1.03, the resulting dimensioned states are scaled appropriately for positions and velocities. The variation is well within the noise of the ephemeris perturbations, and this scaling factor provides a convenient one dimensional degree of freedom that can be very useful in constrained problems such as the present case of searching for ballistic ephemeris capture trajectories. The k scaling technique has proven useful in [33,39].

$$\mathrm{LU}^* = k(\mathrm{LU}) \qquad \mathrm{TU}^* = \sqrt{k^3}(\mathrm{TU}) \qquad \mathrm{VU}^* = \sqrt{1/k}(\mathrm{VU})$$
(8)

Once Eq. (8) is used to unnormalize a state for a given k value, the inertial directions of the instantaneous Jupiter–Europa line and the system angular momentum are used to define a coordinate rotation to the true ephemeris. Equations (9) and (10) provide the mappings for position and velocity vectors. The superscript indicates an unnormalized vector in the RTBP and the subscripts E and J refer to Europa and Jupiter, respectively. It is assumed that the ephemeris velocity of Europa with respect to Jupiter is the time derivative of the ephemeris position (although the position and velocities may in fact be estimated independently, leading to a minor violation of this principle). We also assume that the angular momentum vector, $\boldsymbol{h}_{EJ}$, is a constant although this is not true in general.

$$\boldsymbol{r} = \boldsymbol{R}\boldsymbol{r}^{\mathrm{RTBP}} \qquad \boldsymbol{v} = \dot{\boldsymbol{R}}\boldsymbol{r}^{\mathrm{RTBP}} + \boldsymbol{R}\boldsymbol{v}^{\mathrm{RTBP}}$$
(9)

where

$$\boldsymbol{R} = [\hat{\boldsymbol{x}}|\hat{\boldsymbol{y}}|\hat{\boldsymbol{z}}] \qquad \dot{\boldsymbol{R}} = [\dot{\hat{\boldsymbol{x}}}|\dot{\hat{\boldsymbol{y}}}|\dot{\hat{\boldsymbol{z}}}] \qquad \hat{\boldsymbol{x}} \equiv \frac{\boldsymbol{r}_{EJ}}{r_{EJ}} = \frac{\boldsymbol{r}_E - \boldsymbol{r}_J}{|\boldsymbol{r}_E - \boldsymbol{r}_J|}$$

$$\dot{\hat{\boldsymbol{x}}} = \frac{\boldsymbol{v}_{EJ}}{r_{EJ}} - \frac{\boldsymbol{r}_{EJ}\dot{r}_{EJ}}{r_{EJ}^2} \qquad \hat{\boldsymbol{z}} \equiv \frac{\boldsymbol{h}_{EJ}}{h_{EJ}} = \frac{(\boldsymbol{r}_E - \boldsymbol{r}_J) \times (\boldsymbol{v}_E - \boldsymbol{v}_J)}{|(\boldsymbol{r}_E - \boldsymbol{r}_J) \times (\boldsymbol{v}_E - \boldsymbol{v}_J)|}$$

$$\dot{\hat{\boldsymbol{z}}} \cong 0 \qquad \dot{\hat{\boldsymbol{y}}} = \hat{\boldsymbol{z}} \times \dot{\hat{\boldsymbol{x}}} \qquad \hat{\boldsymbol{y}} \equiv \hat{\boldsymbol{z}} \times \hat{\boldsymbol{x}} \qquad \dot{r}_{EJ} = \boldsymbol{r}_{EJ}^T \boldsymbol{v}_{EJ}/r_{EJ}$$
(10)

The ephemeris positions, velocities, and orientations of the planets and moons are provided by the DE405, jup100, and pck00008.tpc estimated solutions and are publicly available§ from the Jet Propulsion Laboratory (JPL). The active bodies for the ephemeris propagations include the sun, all of the planets, the Earth's moon, and all four Galilean moons. Low degree and order spherical harmonic gravity fields based on Galileo data are considered for Jupiter and Europa. Although the main results of this study are the initial conditions that lead to ballistic ephemeris capture states, the final targeting and optimization is performed with Mystic, a high-fidelity, low-thrust optimization tool under development at the JPL [40]. We

emphasize, however, that Mystic is used only to demonstrate the efficacy of the proposed method. The position, velocity, and epoch that result from the capture design approach can be targeted with any optimizer or differential corrector.

IV. Ballistic Capture Algorithm

An algorithm is described to obtain the initial conditions that lead to a ballistic capture orbit with user-defined characteristics. It is assumed that a provided ephemeris trajectory approaches Europa with appropriate energy and positioning such that a ballistic capture is feasible. Generating the approach trajectory is beyond the scope of this paper. In general it is found using successive resonant flybys of Europa [6–8,11–13,40,41]. The first subsection discusses how to choose a target periodic orbit. Second, the approximate stable manifolds of the periodic orbits are generated, and lastly, the transition is made from the simple to the ephemeris model.

A. Select a Target RTBP Periodic Orbit

As a result of the chaotic nature of the RTBP, a trajectory that approaches Europa in the neighborhood of a ballistic capture orbit can be altered dramatically with small changes in the upstream state. This sensitivity can be exploited to capture directly to orbits with largely varying characteristics for very small fuel expenditures. This is achieved by carefully selecting target unstable periodic orbits that have qualities consistent with a desired capture state. For the case of the Jupiter–Europa system, Russell [30] archives over 616,000 periodic orbits with a variety of defining characteristics. Most of the solutions are unstable and thus have stable manifolds that are candidates for capture orbit applications. The defining qualities associated with each solution include the Jacobi constant, period, characteristic inclination, characteristic radius, minimum altitude, maximum altitude, ratio of the minimum to maximum altitude, and number of xz plane crossings. A database of the solutions is established such that a mission designer can filter all of the characteristics to find a periodic orbit or a range of periodic orbits that are suitable candidates for attracting mechanisms to Europa. (For an electronic copy of the Europa Periodic Orbit Database, send an email request to Ryan.Russell@jpl.nasa.gov. Otherwise, all differential correctors and methods to recreate such a database are described in [30].)

For capture applications with mapping orbit destinations, the most appealing periodic orbits are those that are close to Europa and have near-polar characteristic inclinations and small altitude variations. Other families of orbits such as the Halo, Lisajous, Lyaponov, or combination families have potential application for capture trajectory design. However, in this study we restrict our focus to the highly inclined and highly perturbed two-body orbits to minimize the complexity and cost of spiraling down from the ballistic capture state to the final low-altitude, highly inclined, near-circular science orbit. As mentioned earlier, due to the zero-velocity surface, ballistic captures to highly inclined, near-circular orbits at Europa are not feasible for target orbits with radii less than approximately 5000 km.

Figure 2 illustrates three examples of unstable highly inclined periodic orbits that continuously orbit Europa at energy levels that are feasible for ballistic capture. Table 2 gives the initial conditions and characteristics for each orbit. The solutions are generated using the mass ratio given in Table 1. The direct orbit in Fig. 2c is specifically chosen due to its proximity to a class of highly inclined stable periodic orbits recently identified in [30,33]. Despite the instability of the orbit in Fig. 2c, it is conjectured that the proximity to stable regions will reduce the amount of control authority necessary to fight the perturbations as the spacecraft spirals down to a science orbit [24].

To minimize the time spent in the unstable, high-altitude, highly inclined regions and further minimize the propellant needed to spiral down to the science orbit, it is desirable to choose a target orbit as close to Europa as is feasible.

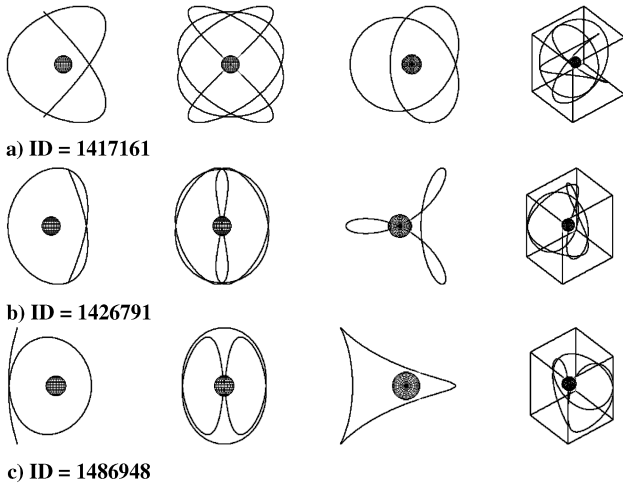a) ID = 1417161

b) ID = 1426791

c) ID = 1486948

Fig. 2 Example unstable periodic orbits useful for designing capture trajectories. From left to right: viewed from 1) negative *y*-axis, 2) positive *x*-axis, 3) positive *z*-axis, and 4) azimuth = −130 deg, elevation = 40 deg.

B. Calculate the Stable Manifolds in RTBP

Once a specific target periodic orbit is selected, the stable manifolds are calculated using the stable eigendirections of the Monodromy matrix as discussed in an earlier section [21]. In Eq. (11), a normalized variable, τ, is introduced that varies from 0 to 1 and parameterizes the periodic orbit across one full period, where t_τ is the time associated with a specific τ, T is the period, and t_0 corresponds to the time associated with a reference state on the periodic orbit.

$$t_\tau = t_0 + \tau T \qquad (11)$$

The Monodromy matrix $\mathbf{\Phi}(T, t_0)$ is integrated once for the reference state $\boldsymbol{X}(t_0)$, and its eigenvalues λ_i and eigenvectors $\boldsymbol{\xi}_i$ are calculated. To proceed, a stable eigenvalue is chosen. Ignoring the unity eigenvalues, an unstable periodic orbit will have at least one and at most two stable eigenvalues where $||\lambda|| < 1$. The eigenvector associated with the chosen stable eigenvalue is the six-dimensional vector direction associated with one of the stable manifolds of the periodic orbit. This vector can be mapped to a different location along the orbit using the state transition matrix as shown in Eq. (12).

$$\boldsymbol{\xi}_\tau = \mathbf{\Phi}(t_\tau, t_0)\boldsymbol{\xi} \qquad (12)$$

The trajectory on the approximated stable manifold that approaches a location on a periodic orbit specified by τ is obtained by integrating backwards in time the conditions given in Eq. (13),

where ε is a normalized scalar that perturbs the state in the direction of the stable eigenvector with a magnitude proportional to the norm of the state. Note that all of the stable eigenvectors considered in this study are real-valued.

$$\boldsymbol{X}' = \boldsymbol{X}(\tau) + \varepsilon ||\boldsymbol{X}(\tau)|| \boldsymbol{\xi}_\tau / ||\boldsymbol{\xi}_\tau|| \qquad (13)$$

The approximated stable manifold then is the set of all trajectories integrated backwards from Eq. (13) for $\tau = 0–1$. As mentioned in an earlier section, the stable manifold from a Halo orbit maintains its tubelike structure at great distances and times from its parent orbit [31]. In such cases, the detailed selection of the perturbing ε value has limited effects on the structure of the resulting estimated manifold. However, for the periodic orbits of interest to this study, i.e., those that close after multiple revolutions, the structure of the approximated manifolds is much less cohesive. Therefore, the selection of the perturbation magnitude plays a significant role in the evolution and the behavior of the resulting trajectories. Note, the perturbation magnitude described in Eq. (13) is simply one of a variety of possible definitions. For example, Gomez et al. [21] illustrate the benefit of scaling the perturbation magnitude with the inverse of the associated eigenvalue.

Table 3 gives a summary of the parameters available for a mission designer to select when approximating a stable manifold for a specific periodic orbit in the RTBP. Note that an invariant manifold can be globally approximated using either parameter ε or τ while holding the other fixed. However, for practical implementation, in terms of generating single trajectories with desired characteristics, we include both as trajectory designing tuning variables. Although unnecessary for capture applications, the generation of the unstable manifolds uses the unstable eigenvectors and integrates forward in time, but otherwise follows an identical procedure.

Figures 3–5 illustrate a set of attracting trajectories for each of the periodic orbits from Fig. 2 for ten equally spaced τ values. Because of xz-plane symmetry, the τ values only vary from 0 to $\frac{1}{2}$. The associated stable eigenvalue is displayed along with the chosen value of ε.

The example approximate manifolds in Figs. 3–5 are calculated using the smallest and therefore the most stable eigenvalue for each of the example orbits. In general, the value of ε is selected to be sufficiently small such that the linear region associated with the state transition matrix is not violated after a few revolutions, but sufficiently large such that the trajectory departs (in backwards time) the vicinity of the periodic orbit in a reasonable time [17,19,21]. An ε value of 0.0001 is generally a good initial guess; this corresponds to roughly a 1 km perturbation in position and 0.1 m/s perturbation in velocity. For the examples shown, ε is varied by several orders of magnitude and a value is selected that leads to a generally cohesive set of attracting trajectories. Note that ε can be a negative value because the eigenvector is simply a direction and does not favor forward or backward. In some cases, but not always, changing the

Table 2   Initial conditions and characteristics[a] of orbits illustrated in Fig. 2

ID	No. of xz plane crossings	x_0, km	v_0, km/s	w_0, km/s	T, days	J, LU^2/TU^2	Inclination[b], deg	Min. altitude, km	Ratio of min:max altitude	ρ[c]
1417161	8	−9872.93624	0.56390318	0.53604013	4.10426372	3.00079	43.5	8312	0.78	65.06
1426791	8	−7266.22483	0.15356112	0.76160114	3.45364150	3.00173	78.6	5706	0.67	36.69
1486948	4	5544.95918	0.10589302	0.85387058	3.07597199	3.00230	82.9	3984	0.43	126.07

[a]Any parameter expressed in unnormalized units is obtained using the length and velocity transformations given in Table 1. Note $y_0 = z_0 = u_0 = 0$.
[b]Characteristic inclination, range is between 0 and 90 deg, equal to $\tan^{-1}(w_0/v_0)$.
[c]ρ is the magnitude of the largest eigenvalue of the Monodromy matrix. Larger values indicate increasing instability. For linear stability, $\rho = 1$.

Table 3   Parameters for generating a stable manifold in the RTBP

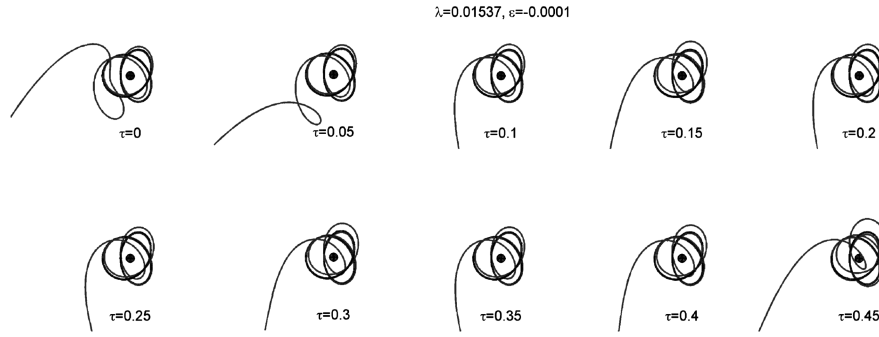| Parameter	Comment
λ_1 or λ_2	Must choose one of the two stable eigenvalues to obtain the eigenvector for manifold calculation.
ε	The scalar perturbing multiplier for eigendirection. Can be positive or negative.
τ	The dimensionless variable that parameterizes the periodic orbit. Can take any value from 0 to 1.

$\lambda=0.01537, \varepsilon=-0.0001$

Fig. 3   Top view of RTBP capture trajectories to periodic orbit in Fig. 2a.

$\lambda=0.027256, \varepsilon=0.0001$
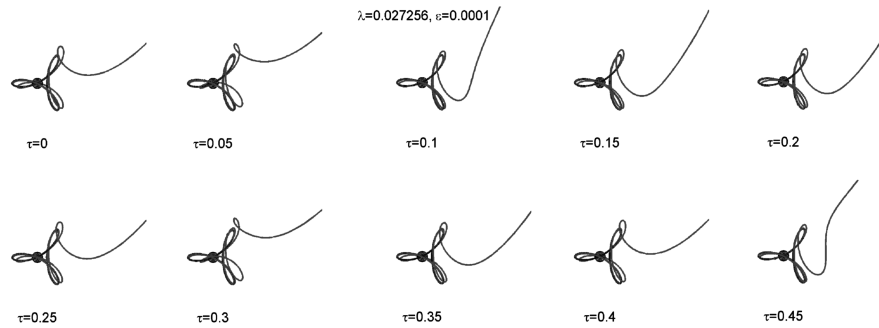
Fig. 4   Top view of RTBP capture trajectories to periodic orbit in Fig. 2b.

$\lambda=0.0079322, \varepsilon=0.0005$
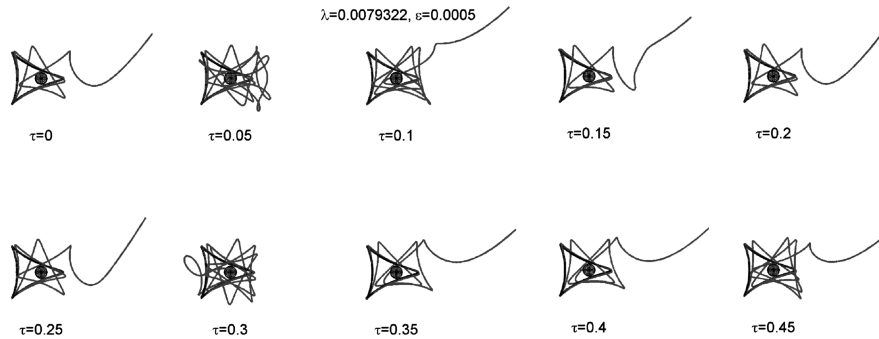
Fig. 5   Top view of RTBP capture trajectories to periodic orbit in Fig. 2c.

$\lambda=0.0079322, \varepsilon=-1e-006$
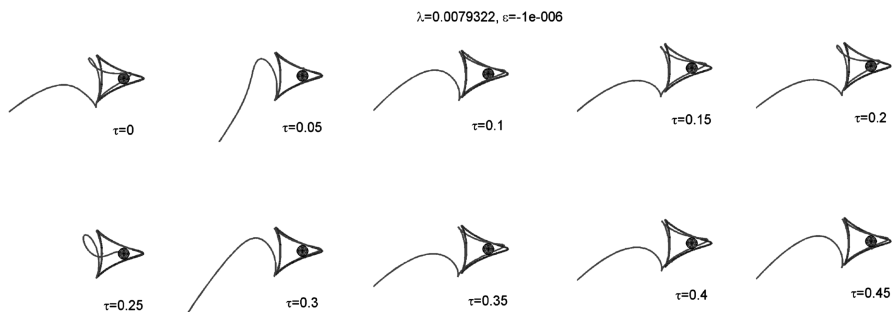
Fig. 6   Same as Fig. 5 except negative ε.

sign on ε can switch the general capture direction to approach from L2 rather than L1 or vice versa as demonstrated in Fig. 6 (in contrast to Fig. 5). Noting that Figs. 3–6 show just the views from above, Fig. 7 illustrates the three-dimensional properties of the example trajectory corresponding to $\tau = 0$ from Fig. 4.

The attracting trajectories to the unstable periodic orbits reveal a diverse set of characteristics that can generally be separated into three categories: trajectories that 1) capture from the left through L1, 2) capture from the right through L2, and 3) capture via a path that impacts the surface. For example, the trajectories in Fig. 3 capture
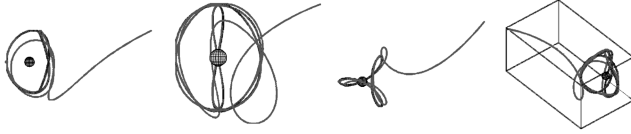
Fig. 7 Different views of attracting trajectory from Fig. 4 ($\tau = 0$).
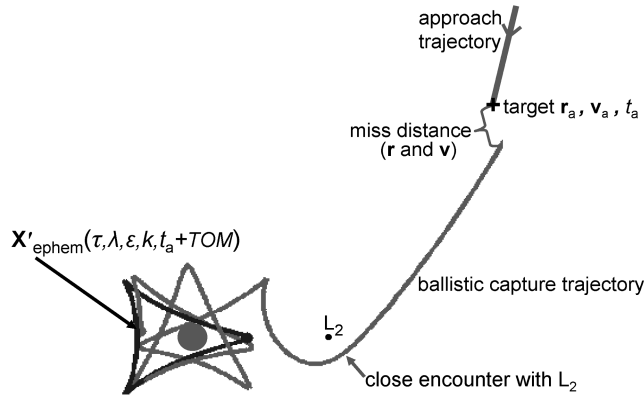

Fig. 8 Capture diagram.

through the L1 region, those in Fig. 4 capture through the L2 region, and the $\tau = 0.05$ and 0.3 trajectories from Fig. 5 capture following an impact. Whereas the third category is useful for surface to periodic orbit applications, we are primarily interested in orbits that approach Europa from beyond its sphere of influence. Noting that Jupiter is on the L1 side of Europa, spacecraft coming from Io require captures that pass near L1, whereas spacecraft coming from Callisto or Ganymede require captures that pass near L2.

C.   Transition to the Ephemeris Model

Once a target RTBP periodic orbit and one of its stable manifolds is estimated, analogous capture trajectories are sought in a realistic ephemeris model. Based on the discussion from an earlier section, the selected approach sacrifices the preservation of the orbit shape for the guarantee of ballistic continuity.

The procedure assumes that a given trajectory approaches Europa with appropriate energy levels such that a ballistic capture is feasible (see Fig. 8). Obtaining such a trajectory will be discussed briefly in the application section to follow. From the ephemeris approach

trajectory, a target seven-state is chosen at a comfortable distance from Europa as depicted in Fig. 8. Several free parameters in the mapping to the ephemeris version of the capture trajectory will be selected to minimize the miss distance of the backward propagated capture trajectory with the target time, position, and velocity on the approach trajectory. Once an ephemeris capture trajectory is found such that the miss distance is reasonably small, the roles of the target and chaser are reversed and the approach trajectory can then be reoptimized to target the seven-state on the ballistic capture trajectory.

The several parameters required for mapping a RTBP capture orbit to the ephemeris model are summarized in Table 4. From Eq. (13), given a τ, ε, and a selection of λ_1 or λ_2, a unique six-state is defined on the RTBP target periodic orbit that departs in reverse time. This perturbed six vector is mapped to the ephemeris using k and Eqs. (8–10), and is applied at the time determined by the target epoch from the approach trajectory plus the free parameter, time spent on the manifold (TOM). Because the ephemeris model is time dependent (as opposed to the RTBP) and the epoch of the state at the end of the approach trajectory remains fixed, the structure of the capture orbit is significantly changed each time TOM is changed. It is therefore an iterative procedure to patch the ballistic capture trajectory with the approach trajectory. The resulting perturbed state in the ephemeris, X'_{ephem}, is a function of all the parameters in Table 4.

Generally, suitable capture trajectories are found by guessing reasonable values for all of the parameters except the k scaling parameter, over which an automated one-dimensional search is performed to minimize the miss distances in position and velocity as indicated in Fig. 8. Values for τ and the eigenvalue are typically chosen based on the RTBP manifolds, and ε and TOM are iterated manually. For the selection of ε, the issue of maintaining the linear assumptions of the state transition matrix is less significant (than in the RTBP case) because the preservation of the parent orbit shape is not the highest priority. The primary concern, however, is to find a completely ballistic, backward propagated single trajectory that originates in the state space vicinity of the approaching orbit. Thus, ε values of 0–0.05 are found to be reasonable guesses. The forward propagation ideally should remain in the vicinity of Europa for several revolutions, but generally the uncontrolled orbit lifetimes are short due to the dominating unstable dynamics.

Figure 9 gives an overview of the algorithm from the selection of the target periodic orbit to the final ephemeris target state that ensures a ballistic capture with the desired characteristics. We emphasize that the algorithm does have several tuning parameters. However, success is not dependent on finding a unique set. Generally, the method leads to a satisfactory design through simple iterations on the

Table 4   Free parameters for the ephemeris model mapping

Parameter	Comment
λ_1 or λ_2	One of the stable eigenvalues.
ε	The scalar perturbing multiplier for eigendirection. Can be positive or negative.
τ	The dimensionless variable that parameterizes the periodic orbit. Can take any value from 0 to 1.
k	The scaling parameter that affects the mapping from the RTBP to the ephemeris and accounts for small variations in the Europa–Jupiter distance.
TOM	Time on the manifold.

Table 5   Resulting states for the example ephemeris capture at Europa

Description	Value[a]
The seven-state selected from the ephemeris approach trajectory that is a priori in the vicinity of a feasible capture in terms of geometry and energy. The subscript a represents approach.	$r_a = (-1.07883310\text{E} + 05, 2.87668841\text{E} + 04, 1.23441619\text{E} + 04)$ km; $v_a = (1.72006636\text{E} + 00, -1.81673502\text{E} + 00, -3.02506277\text{E} - 01)$ km/s; $t_a = 2460919.10489252$ Julian date
The seven-state that results from the optimization of the parameters given in Table 4 for the mapping to ephemeris model. The subscript b represents best.	$r_b = (-1.01918183\text{E} + 05, 3.41628884\text{E} + 04, 1.74521592\text{E} + 04)$ km; $v_b = (1.65707274\text{E} + 00, -1.88920203\text{E} + 00, -5.60147066\text{E} - 02)$ km/s; $t_b = t_a$
The converged state after reoptimizing the approach trajectory given its new target state (r_b, v_b, t_a). The subscript c represents converged.	$r_c = (-1.01919709\text{E} + 05, 3.41616621\text{E} + 04, 1.74520496\text{E} + 04)$ km; $v_c = (1.65708924\text{E} + 00, -1.88923145\text{E} + 00, -5.60167814\text{E} - 02)$ km/s; $t_c = t_a$

[a]Positions and velocities are relative to Europa in the nonrotating J2000 frame.

1) Select an unstable RTBP periodic orbit based on desired capture qualities
2) Propagate the orbit and variational equations for a full period; Record $\mathbf{X}(\tau)$ for $\tau = 0 \rightarrow 1$ and calculate the eigenvectors and eigenvalues of the Monodromy matrix
3) Using the state transition matrix; map and record each of the two stable eigenvectors, $\xi_i(\tau)$ for $\tau = 0 \rightarrow 1$
4) Approximate the stable manifold in RTBP:
   Select λ_1 or λ_2
   Select ε
   FOR $\tau = 0 \rightarrow 1$
   1) Perturb the $\mathbf{X}(\tau)$ state using $\lambda_i, \xi_i(\tau), \varepsilon$ and Eq. (13)
   2) Propagate the perturbed state in reverse time
   3) Plot attracting trajectory
   END τ loop
5) Repeat Step (4) until satisfied with manifold characteristics; Note the τ values that lead to a cohesive set of captures trajectories in RTBP
6) Select a $t_a, \mathbf{r}_a$, and $\mathbf{v}_a$ (epoch, position, and velocity) on a provided ephemeris trajectory that approaches Europa with appropriate energy and geometry
7) Search for ephemeris captures that minimize the miss distance to originating state:
   Select λ_1 or λ_2
   Select ε
   Select τ
   Select TOM
   FOR $k = k_{min} \rightarrow k_{max}$ (typically $0.97 \rightarrow 1.03$)
   1) Perturb the normalized RTBP $\mathbf{X}(\tau)$ state using $\lambda_i, \xi_i(\tau), \varepsilon$, and Eq. (13)
   2) Un-normalize the perturbed state $\mathbf{X}'$ using k, LU^*, VU^*, and Eq. (8)
   3) Map the dimensioned perturbed state to the ephemeris using the epoch, $t_a + TOM$, and the mapping described by Eqs. (9) and (10)
   4) Propagate the new ephemeris state in reverse time from $t = t_a + TOM$ to $t = t_a$, where the end state is $\mathbf{r}, \mathbf{v}$
   5) Calculate and store the miss distances $\|\mathbf{r} - \mathbf{r}_d\|$ and $\|\mathbf{v} - \mathbf{v}_d\|$
   END k loop
   Record $\mathbf{r}_b$ and $\mathbf{v}_b$: the $\mathbf{r}$ and $\mathbf{v}$ associated with the best miss distances
8) Repeat Step (7) until satisfied with the ballistic ephemeris capture trajectory
9) Re-optimize the approach trajectory to target the $\mathbf{r}_b$ and $\mathbf{v}_b$ at time t_a to a satisfactory tolerance (~10 km, 0.1 m/s)
10) Store the converged state as $\mathbf{r}_c$ and $\mathbf{v}_c$
11) Propagate the converged state to a ballistic capture
12) After a few revs around Europa, employ low-thrust to stabilize the trajectory and commence a spiral down to the science orbit

Fig. 9   Ballistic ephemeris model capture algorithm.

parameters. Whereas it is possible to select all of the parameters via a formal optimization code, the described simple approach is found to be sufficient. The following section demonstrates the algorithm with a low-thrust transfer from Ganymede to Europa ending in a highly inclined, near-circular orbit about Europa.

V.   Application: Low-Thrust Ganymede to Europa Transfer

The algorithm from Fig. 9 is applied to search for a seven-state that leads to a ballistic ephemeris capture at Europa. The target periodic orbit, ID = 1486948, is chosen and illustrated in Fig. 2c. This orbit
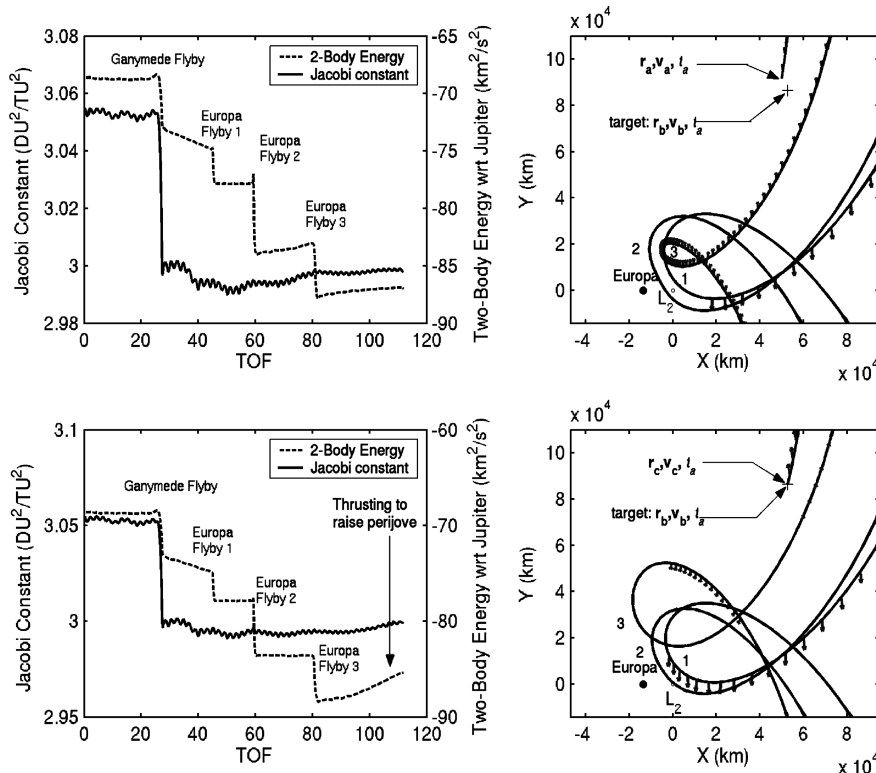

Fig. 10   Example low-thrust ephemeris transfer from Ganymede to the vicinity of Europa. Arrows on the trajectory indicate thrusting. Top row: initial guess. Bottom row: converged trajectory that leads to a ballistic capture when propagated further. See Table 5 for relevant states.

has mean two-body eccentricity, inclination, and semimajor axis near 0.2, 65 deg, and 8500 km, respectively. Its instability due to the high inclination makes it a difficult target for traditional optimization or targeting tools. Steps 1–5 of the algorithm are performed and result in plots similar to Fig. 5. For $\lambda = \lambda_1 (0.0079322)$, it is clear that several values of τ and ε lead to capture trajectories through L2. Next, the ephemeris approach trajectory is designed according to step 6.

In this example, the approach trajectory is a low-thrust transfer that originates on an escape path from Ganymede. To take advantage of the manifold design philosophy using limited control, the approach trajectory must be designed with careful energy and geometry considerations. In general, if the approach trajectory is on or near the *intermoon superhighway*, or the dominating stable manifold associated with the Halo family, it is relatively easy to make minor control adjustments to target the specific capture trajectory of interest. However, with limited control it often is not feasible to target a specific close capture trajectory if starting on an approach with energy and geometry appropriate for an entirely different class of orbits, such as a typical DRO type capture [8].

To ballistically capture at Europa, it is a necessary (but not sufficient) condition to have the same Jacobi energy as the target periodic orbit. To achieve the Jacobi energies representative of the orbits in Fig. 2, thrusting is typically required. However, for limited fuel missions, it is often possible to combine minor thrusting with a string of successive flybys of various bodies to manipulate the geometry, phasing, and energy levels to suit specific mission needs. The leveraging from the flybys is controlled by the minimum altitudes, where the smaller altitudes yield larger control. However, for successive flyby encounters with the same body, thrusting is required to significantly raise or lower minimum altitudes from one flyby to the next. Because the final approach before capture generally requires a close encounter with L1 or L2 rather than the capture body itself, a balance of thrusting and *resonant hopping* via successive flybys is typically required to set up a low-energy capture of Europa or any planetary moon. For more detail see [6,7].

The initial guess for the approach trajectory in the present example is shown on the top row of Fig. 10. The trajectory consists of one Ganymede flyby and three Europa flybys before the final approach. The two-body energy with respect to Jupiter and the Jacobi constant with respect to Europa histories are illustrated. The flybys and intermediate thrusting are used to target appropriate energy and geometry for a ballistic capture. Note, in the unthrusted case these energy values are only approximately constant in the full ephemeris model. Going back to step 6 from the algorithm, the state $\boldsymbol{r}_a$, $\boldsymbol{v}_a$, and t_a is selected as a target for the optimization of the ephemeris mapping. The optimization in steps 7 and 8 are performed and the best resulting state, $\boldsymbol{r}_b$ and $\boldsymbol{v}_b$, that leads to an ephemeris capture is illustrated in Fig. 11. The optimized parameters include: target periodic orbit ID = 1486948, $\lambda = \lambda_1 (0.0079322)$, $\epsilon = 0.03$, $\tau = 0.2$, TOM= 6.1 day, and $k = 1.0053947$. Note the resemblance to its corresponding RTBP trajectory in Fig. 5 ($\tau = 0.2$).

Next, from step 9, the full approach trajectory from Ganymede is retargeted and reoptimized with Mystic using the new target state $\boldsymbol{r}_b$ and $\boldsymbol{v}_b$. The resulting trajectory converges to the final state $\boldsymbol{r}_c$ and $\boldsymbol{v}_c$
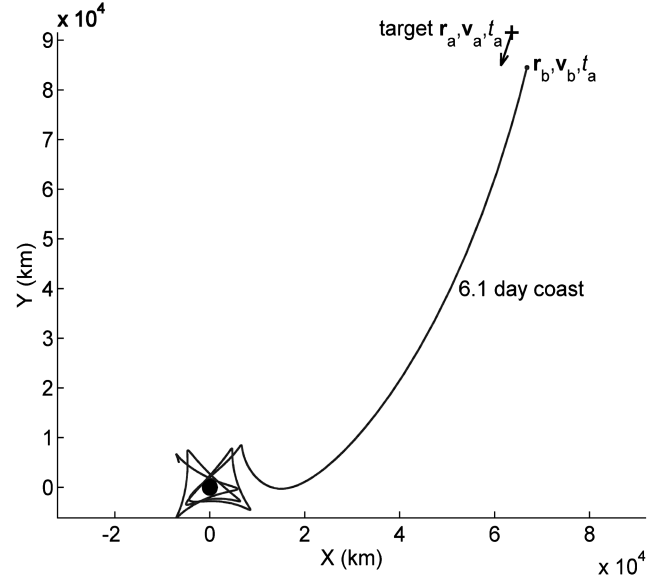

Fig. 11 Ephemeris ballistic capture trajectory resulting from algorithm given in Fig. 9.

within 2 km in position and 4 cm/s in velocity. Although the trajectories are highly sensitive in nature, tolerances of 10 km and 10 cm/s are generally sufficient to maintain the desired structure of the capture. For a better understanding of the appropriate tolerances, Poincaré maps similar to those described in [32] would prove useful. The converged approach trajectory and energy histories are illustrated in the bottom row of Fig. 10. Note, the optimizer primarily adjusts the third Europa flyby and raises perijove with thrusting before the final approach.

Finally, the trajectory design is completed by ballistically propagating the converged final approach state to a close, highly inclined capture state about Europa. Following a ballistic coast that captures through L2 and completes a full revolution around Europa, low thrust again is used to maintain the orbit and start the spiral down towards the science orbit. Figure 12 illustrates the final optimized trajectory that includes a ballistic 2.3 day ephemeris capture and 4.3 days of optimized low-thrust maneuvers (acceleration ~ 0.13 mm/s^2). The resulting near two-body orbit has eccentricity ~ 0.003, inclination ~ 71 deg, and semimajor axis ~ 7280 km. The continuation to the science orbit is omitted for clarity although it is straightforward to implement.

As illustrated in [7,8], it is difficult to control highly inclined, low-thrust capture trajectories at Europa. Thus, the resulting orbits are generally erratic in shape, making them difficult to reproduce across different epochs or ephemeris files. On the contrary, note the structure of the capture orbit in Fig. 12 is well-behaved despite existing in a highly chaotic and unstable region. Whereas the final capture orbits are clearly dependent on both the epoch and ephemeris, the basic characteristics of the orbits are generally
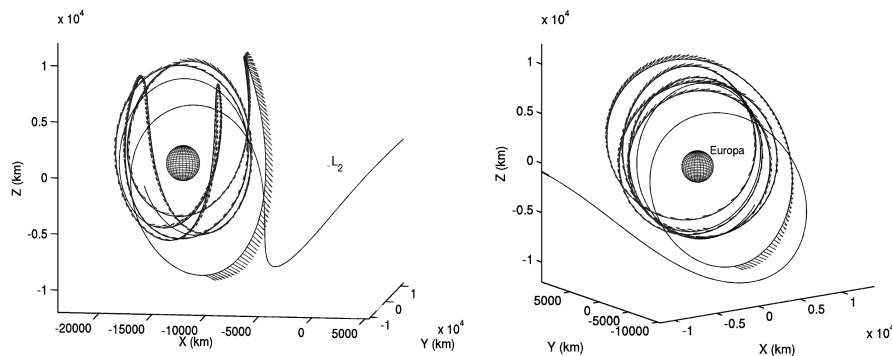

Fig. 12 Continuation of the converged trajectory from Fig. 10. Left: rotating frame. Right: nonrotating frame. Note the smooth, controlled capture.

reproducible because the technique is based largely on the time invariant model of the RTBP. The Δv requirement of the presented example is similar to the lowest Δv high-inclination capture examples in [7,8].

VI. Conclusions

A dynamical systems approach is applied to the design of low-energy capture trajectories at Europa. A database of periodic orbits around Europa is queried to find target unstable orbits with user-specified characteristics such as altitude and inclination. The approximate stable manifolds of several example target periodic orbits are investigated, documented, and subsequently used as attracting mechanisms for capture. The subtleties associated with mapping these simple model manifolds into a realistic model are explored and an algorithm is presented to find and target efficient ballistic captures using a full ephemeris. The presented technique is systematic and allows a mission designer to target specific characteristics of a capture state using little control authority even in the notably unstable environments such as highly inclined orbits about Europa. Because the method is based on the time invariant simplified model, the resulting capture trajectories are robust to design changes associated with different epochs and ephemeris models. Although close capture trajectories around Europa are the focus of this paper, the technique is applicable for ephemeris captures in any system that is well approximated by the restricted three-body model.

Acknowledgments

References

[1] Scheeres, D. J., Guman, M. D., and Villac, B. F., "Stability Analysis of Planetary Satellite Orbiters: Application to the Europa Orbiter," *Journal of Guidance, Control, and Dynamics*, Vol. 24, No. 4, 2001, pp. 778–787.

[2] Lara, M., and San-Juan, J. F., "Dynamic Behavior of an Orbiter Around Europa," *Journal of Guidance, Control, and Dynamics*, Vol. 28, No. 2, 2005, pp. 291–297.

[3] Aiello, J., "Numerical Investigation of Mapping Orbits About Jupiter's Icy Moons," AAS Paper 2005-377, Aug. 2005.

[4] Lam, T., and Whiffen, G. J., "Exploration of Distant Retrograde Orbits around Europa," AAS Paper 05-110, Jan. 2005.

[5] Paskowitz, M. E., and Scheeres, D. J., "Transient Behavior of Planetary Satellite Orbiters," AAS Paper 05-358, Aug. 2005.

[6] Whiffen, G. J., "An Investigation of a Jupiter Galilean Moon Orbiter Trajectory," AAS Paper 03-544, Aug. 2003.

[7] Whiffen, G. J., "Jupiter Icy Moons Orbiter Reference Trajectory," AAS Paper 06-186, 2006.

[8] Lam, T., and Hirani, A. N., "Characteristics of Transfers to and Captures at Europa," AAS Paper 06-188, 2006.

[9] Koon, W. S., Lo, M. W., Marsden, J. E., and Ross, S. D., "The Genesis Trajectory and Heteroclinic Connections," AAS Paper 99-451, Aug. 1999.

[10] Koon, W. S., Lo, M. W., Marsden, J. E., and Ross, S. D., "Low Energy Transfer to the Moon," *Celestial Mechanics and Dynamical Astronomy*, Vol. 81, Nos. 1–2, Sept. 2001, pp. 63–73.

[11] Lo, M. W., Anderson, R. L., and Whiffen, G. J., "The Role of Invariant Manifolds in Low Thrust Trajectory Design," AAS Paper 04-228, Feb. 2004.

[12] Anderson, R. L., and Lo, M. W., "The Role of Invariant Manifolds in Low Thrust Trajectory Design (Part 2)," AIAA Paper 2004-5305, Aug. 2004.

[13] Lo, M. W., Anderson, R. L., Lam, T., and Whiffen, G., "The Role of Invariant Manifolds in Low Thrust Trajectory Design (Part 3)," AAS Paper 06-190, Jan. 2006.

[14] Lo, M. W., and Parker, J. S., "Unstable Resonant Orbits Near Earth and Their Applications in Planetary Missions," AAS Paper 04-5304, Aug. 2004.

[15] Gómez, G., Koon, W. S., Lo, M. W., Marsden, J. E., Masdemont, J., and Ross, S. D., "Connecting Orbits and Invariant Manifolds in the Spatial Restricted Three-Body Problem," *Nonlinearity*, Vol. 17, No. 5, Sept. 2004, pp. 1571–1606.

[16] Gómez, G., Koon, W. S., . Lo, M. W., Marsden, J. E., Masdemont, J., and Ross, S. D., "Invariant Manifolds, The Spatial Three-Body Problem and Space Mission Design," AAS Paper 01-301, July 2001.

[17] Senet, J., and Ocampo, C., "Low-Thrust Variable Specific Impulse Transfers and Guidance to Unstable Periodic Orbits," *Journal of Guidance, Control, and Dynamics*, Vol. 28, No. 2, 2005, pp. 280–290.

[18] Serban, R., Koon, S. K., Lo, M. W., Marsden, J. E., Petzold, L. R., Ross, S. D., and Wilson, R. S., "Halo Orbit Mission Correction Maneuvers Using Optimal Control," *Automatica*, Vol. 38, No. 4, April 2001, pp. 571–583.

[19] Howell, K. C., Barden,, B. T., and Lo, M. W., "Application of Dynamical Systems Theory to Trajectory Design for a Libration Point Mission," *The Journal of the Astronautical Sciences*, Vol. 45, No. 2, April–June 1997, pp. 161–178.

[20] Belbruno, E., "A Low Energy Lunar Transportation System Using Chaotic Dynamics," AAS Paper 05-382, Aug. 2005.

[21] Gomez, G., Llibre, J., Martinez, R., and Simo, C., *Dynamics and Mission Design Near Libration Points. Vol. 1 Fundamentals: The Case of Collinear Libration Points*, Vol. 2, World Scientific Monograph Series in Mathematics, World Scientific, Singapore, 2001, pp. 148, 150–153.

[22] Belbruno, E., and Miller, J., "Sun-Perturbed Earth-to-Moon Transfers with Ballistic Capture," *Journal of Guidance, Control, and Dynamics*, Vol. 16, No. 4, 1993, pp. 770–775.

[23] Lo, M. W., "The Lunar L1 Gateway: Portal to the Stars and Beyond," AIAA Paper 2001-4768, 2001.

[24] Villac, B., and Lara, M., "Stability Maps, Global dynamics, and Transfers," AAS Paper 05-378, Aug. 2005.

[25] Farquhar, R. W., Muhonen, D. P., Newman, C. R., and Heuberger, H. S., "Trajectories and Orbital Maneuvers for the First Libration Point Satellite," *Journal of Guidance, Control, and Dynamics*, Vol. 3, No. 6, 1980, pp. 549–554.

[26] Sharer, P., and Harrington, T., "Trajectory Optimization for the ACE Halo Orbit Mission," AAS Paper 96-3601, July 1996.

[27] Dunham, D. W., Jen, S. J., Roberts, C. E., Seacord, A. W., II, Sharer, P. J., Folta, D. C., and Muhonen, D. P., "Transfer Trajectory Design for the SOHO Libration-Point Mission," IAF Paper 92-0066, Sept. 1992.

[28] Koon, W. S., Lo, M. W., Marsden, J. E., and Ross, S. D., "The Genesis Trajectory and Heteroclinic Connections," AAS Paper 99-451, Aug. 1999.

[29] Howell, K. C., Barden,, B. T., Wilson, R. S., and Lo, M. W., "Trajectory Design Using a Dynamical Systems Approach with Applications to Genesis," AAS Paper 97-709, Aug. 1997.

[30] Russell, R. P., "Global Search for Planar and Three-Dimensional Periodic Orbits Near Europa," *Journal of the Astronautical Sciences* (to be published).

[31] Hirani, A. H., and Lo, M. W., "Surface Structure of an Invariant Manifold of a Halo Orbit," AAS Paper 2005-379, Aug. 2005.

[32] Paskowitz, M. E., and Scheeres, D. J., "Robust Capture and Transfer Trajectories for Planetary Satellite Orbiters," *Journal of Guidance, Control, and Dynamics*, Vol. 29, No. 2, 2006, pp. 342–353.

[33] Lara, M., Russell, R. P., and Villac, B., "On Parking Solutions Around Europa," AAS Paper 05-384, Aug. 2005.

[34] Bagenal, F., Dowling, T., and McKinnon, W. (eds.), *Jupiter, The Planet, Satellites, and Magnetosphere*, Cambridge Planetary Society, Cambridge, England, U.K., 2004, pp. 36, 347.

[35] Szebehely, V., *Theory of Orbits. The Restricted Problem of Three Bodies*, Academic Press, New York, 1967, Chap. 1.

[36] Battin, R. H., *An Introduction to the Mathematics and Methods of Astrodynamics*, American Institute of Aeronautics and Astronautics, New York, 1987, p. 453.

[37] Nayfeh, A. H., and Balachandran, B., *Applied Nonlinear Dynamics*, John Wiley and Sons, New York, 1995, Sec. 3.2.

[38] Broucke, R., "Stability of Periodic Orbits in the Elliptic, Restricted Three-Body Problem," *AIAA Journal*, Vol. 7, No. 6, 1969, pp. 1003–1009.

[39] Lara, M., and Russell, R. P., "On the Computation of a Science Orbit About Europa," *Journal of Guidance, Control, and Dynamics* (to be published).

[40] Whiffen, G. J., and Sims, J. A., "Application of the SDC Optimal Control Algorithm to Low-Thrust Escape and Capture Trajectory Optimization," AAS Paper 02-208, 2002.

[41] Johannesen, J., and D'Amario, L. A., "Europa Orbiter Mission Trajectory Design," AAS Paper 99-360, Aug. 1999.